ACS APPLIED MATERIALS & INTERFACES

Research Article

www.acsami.org

Assembly and Function of the tRNA-Modifying GTPase MnmE Adsorbed to Surface Functionalized Bioactive Glass

C. Gruian,[†,‡] S. Boehme,[‡] S. Simon,[†] H.-J. Steinhoff,[‡] and J. P. Klare*[,‡]

[†]Faculty of Physics and Institute of Interdisciplinary Research in Bio-Nano-Sciences, Babes-Bolyai University, Cluj-Napoca, 400084, Romania

[‡]Department of Physics, University of Osnabrück, Osnabrück, 49069, Germany

Supporting Information

ABSTRACT: Protein adsorption onto solid surfaces is a common phenomenon in tissue engineering related applications, and considerable progress was achieved in this field. However, there are still unanswered questions or contradictory opinions concerning details of the protein's structure, conformational changes, or aggregation once adsorbed onto solid surfaces. Electron paramagnetic resonance (EPR) spectroscopy and site-directed spin labeling (SDSL) were employed in this work to investigate the conformational changes and dynamics of the tRNA-modifying dimeric protein MnmE from *E. coli*, an ortholog of the human GTPBP3, upon adsorption on bioactive glass mimicking the composition of the classical 45S5 Bioglass. In addition, prior to protein attachment, the bioactive glass surface was modified with the protein coupling agent glutaraldehyde. Continuous wave EPR spectra of different spin labeled MnmE mutants were recorded to assess the dynamics of the attached spin labels before and after protein adsorption. The area of the continuous wave (cw)-EPR absorption spectrum was further used to determine the amount of the attached protein. Double electron-electron resonance (DEER) experiments were conducted to measure distances between the spin labels before and after adsorption. The results revealed that the contact regions between MnmE and the bioactive glass surface are located at the G domains and at the N-terminal domains. The low modulation depths of all DEER time traces recorded for the adsorbed single MnmE mutants, corroborated with the DEER measurements performed on MnmE double mutants, show that the adsorption process leads to dissociation of the dimer and alters the tertiary structure of MnmE, thereby abolishing its functionality. However, glutaraldehyde reduces the aggressiveness of the adsorption process and improves the stability of the protein attachment.

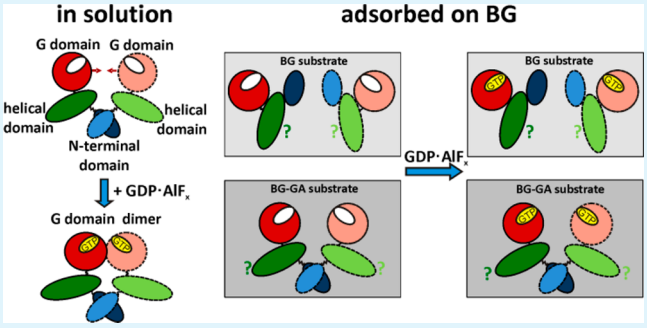

KEYWORDS: *bioglass, MnmE, protein adsorption, glutaraldehyde, biocompatibility, site-directed spin labeling, EPR spectroscopy*

INTRODUCTION

The biological functions of proteins, enzymes, and other biological molecules are associated with structural dynamics and are often realized by changes in conformation. A major interest in biology is to understand the function of biomacromolecules, in order to establish how a biological process proceeds from simple structural changes in biomolecules to the final and often complex biological function. In this respect, information concerning kinetics, structure, and conformational dynamics of biomacromolecules is of primary importance. Besides the information about their behavior in the native environment, for optimal performance in biomedical or physiological applications, it is important to investigate how complex biomolecules change their structure when interacting with foreign materials and surfaces. For example, adsorption of protein molecules onto solid surfaces plays a key role in many natural processes and frequently results in conformational and orientation changes within the adsorbed layer.[1,2] An intensive knowledge of the protein adsorption process is not only beneficial for optimization of the surface structure of biomaterials but also helpful to develop specific applications within the field of biomedicine.[3] In particular, protein adsorption on osteoinductive bioceramic type surfaces was extensively studied in the past years since it plays a vital role during bone tissue regeneration[4,5] and helps in understanding the mechanisms of bioactivity.[6−8] Several experimental and theoretical approaches recently reported that adsorbed proteins can also influence surface mineralization of the substrate by affecting the nucleation and growth as well as the morphology, size, and orientation of Ca−P crystals.[9−11] Proteins are spontaneously adsorbed onto bioactive glass (BG), long before Ca−P precipitation; actually, the first processes that occur at the BG surface upon immersion in simulated body fluid (SBF) are ion release (dissolution) and SBF diffusion.[12,13] Notwithstanding, details concerning protein structure and dynamics after adsorption, the exact amount of the protein attached to

Received: February 13, 2014
Accepted: May 1, 2014
Published: May 1, 2014

   dx.doi.org/10.1021/am500933e | ACS Appl. Mater. Interfaces 2014, 6, 7615−7625

the substrate, and the mechanisms of adsorption need to be further clarified.[3,14] The biological and physico-chemical methods that have been widely used in research on protein adsorption on solid materials so far present difficulties in obtaining detailed structural and dynamic information for the adsorbed proteins.

In the present work, we used site-directed spin labeling (SDSL)[15−18] in combination with electron paramagnetic resonance (EPR) spectroscopy to investigate the conformational changes the tRNA-modifying protein MnmE undergoes upon adsorption on the solid surface of a BG. MnmE is an GTP-hydrolyzing (G) protein conserved between bacteria and eukarya, belonging to the expanding class of G proteins activated by nucleotide-dependent dimerization (GADs).[19] The protein is involved in the biosynthesis of a hypermodified nucleotide (nucleoside 5-methyl-aminnomethyl-2-thiouridine), which plays an important role in the structure and function of transfer ribonucleic acids.[20] The human ortholog of MnmE, hGTPBP3, has been implicated in the development of severe mitochondrial myopathies such as MERRF (myoclenic epilepsy ragged red fibers), MELAS (mitochondrial encephalomyopathy lactic acidosis stroke), and nonsyndromic deafness.[21−24] The crystal structure of the MnmE dimer (pdb 1XZP, from *Thermotoga maritima*) reveals that each monomer consists of three domains: an N-terminal domain responsible for constitutive dimerization, a central helical domain, and the G domain.[25] On the basis of the available crystal structures and using SDSL and double electron-electron resonance (DEER) spectroscopy,[25−27] it has already been shown that in the nucleotide-free state the G domains face each other with their nucleotide binding sites (Figure 1) without displaying any structural contacts between each other.[26] In the presence of GDP·AlF_x, a transition state mimic for GTP hydrolysis, the G domains contact each other by overcoming a 20−30 Å distance gap.[26] The multi-domain architecture and the observed large conformational change occurring upon activation renders this protein an ideal model system to study the influence of protein-BG interaction on functional conformational dynamics. The present study will thus focus on changes induced in the MnmE structure by the adsorption process in two steps of its GTPase cycle: the apo-state and the GTP hydrolysis transition (GDP·AlF_x bound) state. It was recently shown that interaction between MnmE and this type of BG causes severe aggregation of the protein β-sheet type structure; however, it could also be shown that the use of GA decreased the degree of protein denaturation.[30]

The most decisive factors concerning the protein adsorption process are the physico-chemical features of the material's surface. In the case of large biomolecules such as proteins or enzymes, the adsorption process is driven by surface energy, hydrophobicity, intermolecular forces, and ionic or electrostatic interactions. As a result of all these factors, proteins tend to unfold upon adsorption, so that their internal regions form additional contacts with the foreign solid surface.[29] For the present work, the surface of the BG substrate was silanized with 3-aminopropyl-triethoxysilane (APTS) and subsequently modified with the protein coupling agent glutaraldehyde (GA) to facilitate protein adsorption.[30,31] This commonly used functionalization process modifies surface hydrophobicity and texture. The question is how these factors influence the structure of adsorbed protein and the efficiency of the adsorption process.

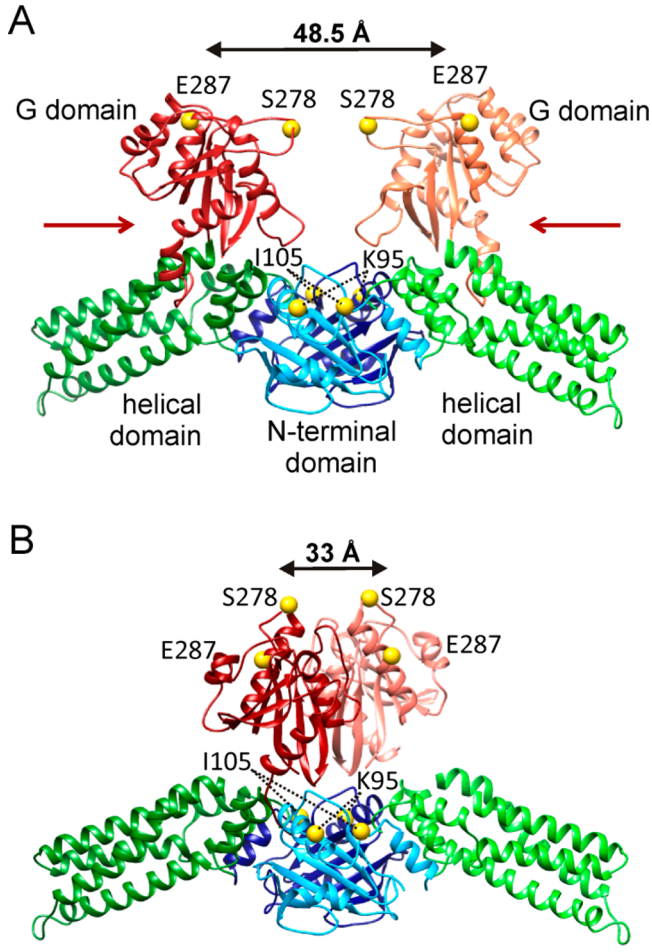

Figure 1. Crystal structure of the MnmE homodimer in apo-state (A), generated with pdb 1XZP[25]), and GDP·AlF_x bound state (B, pdb 2GJ8[27]). Positions of the native residues that were mutated to cysteines (E287, S278, I105, and K95) and spin labeled with MTSSL are indicated by yellow spheres. Upon GTP hydrolysis, the G domains move by approximately 15.5 Å, from 48.5 to 33 Å (measured for the Cα-Cα positions of the first P-loop glycines).[26]

The method used in this study (SDSL EPR) is able to provide both, detailed structural and dynamic information about the labeled biomolecules, with a spatial resolution at the level of backbone fold.[32] The method is complementary to X-ray crystallography and NMR spectroscopy, being widely applicable for investigations on a protein's structure and conformational dynamics.[33,34] Recent studies furthermore showed that this method can be extended to proteins encapsulated[35] in or adsorbed on solid surfaces,[36,37] thus permitting investigation of adsorption-induced conformational changes with high spatial resolution. SDSL involves the introduction of a spin label side chain at a specific site in the amino acid sequence by cysteine substitution mutagenesis followed by modification of the sulfhydryl group with a nitroxide reagent[17] (Figure 2). In our experiments, the amino acids at four positions within MnmE were mutated to cysteine and subsequently spin labeled with the (1-oxyl-2,2,5,5-tetramethyl-3-pyrroline-3-methyl) methanethiosulfonate spin label (MTSSL): Ser278 and Glu287 (both located in the G domain); Ile105 and Lys95 (both situated in the N terminal domain of the protein) (see Figure 1). To characterize the dynamics of the G domains upon interaction with the BG

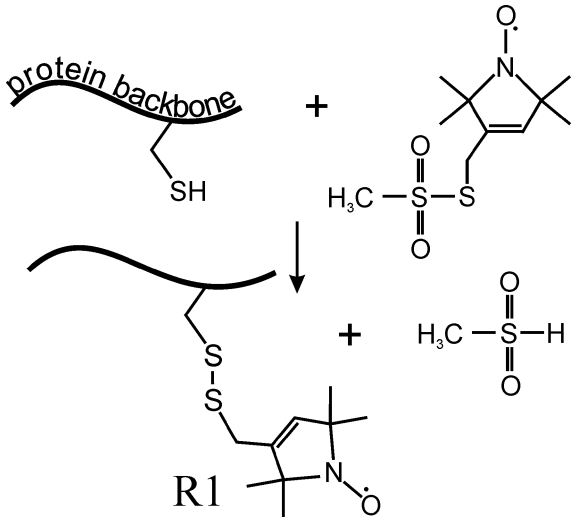

Figure 2. Reaction of the (1-oxyl-2,2,5,5-tetramethyl-3-pyrroline-3-methyl) methanethio-sulfonate spin label with the sulfhydryl group of a cysteine side chain, generating the spin label side chain R1.

surface, continuous wave (cw) and pulse EPR experiments were conducted on the single mutants and on the double mutant Ser278R1-Ile105R1 in the apo-state and GDP·AlF_x bound states before and after adsorption on the BG (R1 denotes the MTSSL side chain). cw EPR spectroscopy was used to investigate the dynamics of the spin labels at room temperature in order to achieve information about the putative immobilization of the protein on the BG surface and to identify conformational changes that are likely to appear in the spin labels local environment upon adsorption. DEER spectroscopy was employed to determine distances between the two spin labels in the MnmE dimer (in the frozen state at 50 K) before and after adsorption onto BG, thereby providing global information about changes in protein dynamics and tertiary structure upon adsorption. From the DEER data, it was also possible to quantify the remaining fraction of MnmE dimers after adsorption.

MATERIALS AND METHODS

If not noted otherwise, chemicals were obtained from Sigma-Aldrich (Munich, Germany).

BG Preparation. The BG used as substrate was prepared by the sol gel method, with the following composition (in mol %): 45% SiO_2, 24.5% Na_2O, 24.5% CaO, and 6% P_2O_5 (identical with the classical 45S5 Bioglass). As starting reagents, tetraethoxysilane (TEOS), $Ca(NO_3)_2{\cdot}4H_2O$, $(NH_4)_2{\cdot}HPO_4$, and Na_2CO_3 were used. The sample was aged for 30 days at room temperature and then dried at 310 °C in air for 1 h. The particles size distribution was determined using a Shimadzu Nano Particle Size Distribution Analyzer SALD-7101, applying the laser diffraction method with a UV semiconductor laser (375 nm wavelength). The particle size of the milled BG ranged from hundreds of nm to a few μm (Figure 3). Static contact angle measurements with distilled water were performed on the BG surface before milling, by using the sessile drop method where the angle was determined from the tangent made to the drop curvature at the base. The obtained water contact angle value was 41°, indicating the hydrophobic character of the BG surface after preparation.[38,39]

The BG particles were silanized with 3-aminopropyl-triethoxysilane (APTS) and subsequently modified with GA following the protocol presented in other studies.[30,31] First, the BG was immersed for 4 h into an aqueous APTS solution (0.45 mol/L, pH adjusted to 8 by adding 1 M HCl) at 80 °C. After 4 h, the sample was collected, washed in deionized water, then immersed for 1 h in 1 M (9.6% w/v) GA solution at room temperature, and finally washed again in deionized water.

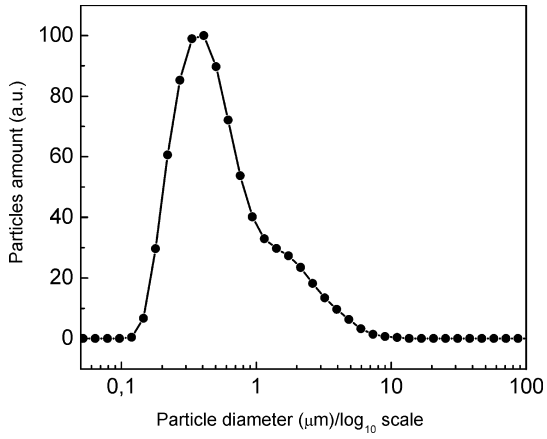

Figure 3. Bioactive glass particle size distribution obtained by the laser diffraction method.

A Sorptomatic 1990 instrument (Thermo Scientific, Germany) was used for the textural characterization of the substrate before and after surface functionalization, on the basis of the Brunauer–Emmet–Teller (BET) theory for multilayer adsorption of nitrogen. Prior to nitrogen adsorption, all samples were degassed in vacuum at 119 °C for 2 h. The specific surface area for the BG substrate was determined to be 291 m^2/g after preparation and 139 m^2/g after functionalization with GA.

Spin Labeling. The purified, nucleotide-free single Cys-mutants of *E. coli* MnmE Ser278 (S278), Glu287 (E287), Ile105 (I105), and Lys95 (K95) and the double mutant Ser278-Ile105 (S278-I105), prepared as described before,[26] were incubated with 10 mM dithiothreitol (DTT) (4°C, 2 h). Buffer conditions were 100 mM KCl, 50 mM Tris-DCl (pH 7.5), and 5 mM $MgCl_2$ in D_2O. DTT was removed by repeated dilution steps with buffer, using centrifugal filter units with 30 kDa molecular weight cut-off (Amicon/Millipore, Carringtwohill, Co. Cork, Ireland). Afterwards, the protein solutions were incubated with a 6-fold molar excess of MTSSL (Toronto Research; Alexis Biochemicals) for 16 h (4°C). The unbound free MTSSL was removed by repeated ultrafiltration as described above. Labeling efficiencies were estimated to be >50% in all cases. In the following, the spin labeled mutants will be denoted as S278R1, E287R1, I105R1, K95R1, and S278-I105R1.

Protein Adsorption. Powder samples (30 mg) were incubated for 2 h at room temperature in a 150 μL solution of spin labeled MnmE with protein concentrations of ~300 μM (~15 mg/mL). Buffer conditions were as mentioned in the previous section. X-ray diffraction and Fourier transform IR spectroscopic analyses (see Supporting Information) of samples immersed for 2 h in buffer solution confirmed that during the protein adsorption process no recognizable surface mineralization occurs, that would alter the properties of the substrate's surfaces. Unless noted otherwise, incubation with the transition state analogue GDP·AlF_x was performed after protein adsorption. Briefly, approximately 200 μM of nucleotide-free spin labeled *E. coli* MnmE, already adsorbed on BG, was incubated in 1 mM GDP, 1 mM $AlCl_3$, and 50 mM NaF in the buffer conditions described above.

To verify the efficiency of the adsorption process on each substrate, samples containing the E287R1 mutant attached to pristine and GA functionalized BG were ultrasonicated for 45 min at room temperature and then washed again with buffer solution to remove the protein detached from the surface. Afterwards, the samples were examined again at room temperature by cw-EPR spectroscopy.

cw-EPR Measurements. X-band cw-EPR experiments were performed using a home-made EPR spectrometer equipped with a Bruker dielectric resonator. The microwave power was set to 1.0 mW; the B-field modulation amplitude was 0.15 mT. Glass capillaries of 0.9 mm inner diameter were filled with 15 μL of the samples, considering

that the EPR active volume of the sample tube was 10 μL. The second integral of the cw-EPR signals (1st derivative absorption spectra) was directly proportional to the spin concentration in the sample and was used to calculate the amount of protein attached onto the bioactive glass. 2,2,6,6-Tetramethyl-1-piperidinyloxy (TEMPO) at a concentration of 100 μM was used as a reference spin probe. In order to have reliable comparison of the protein amounts attached on the two substrates, the filled capillaries were centrifuged for 10 min at 3725 rcf to ensure the same sample density in each tube.

DEER Measurements. DEER measurements were accomplished at X-band frequencies (9.3-9.4 GHz) with a Bruker Elexsys 580 spectrometer equipped with a Bruker Flexline split-ring resonator ER 4118XMS3 and a continuous flow helium cryostat ESR900 (Oxford Instruments) controlled by an Oxford Intelligent temperature controller ITC 503S. Prior to freezing the protein in 3 mm inner diameter EPR tubes, 12.5 % deuterated glycerol was added to each sample. Measurements were performed using the four-pulse DEER sequence:[40,41]

$$\pi/2(\nu_{obs}) - \tau_1 - \pi(\nu_{obs}) - t' - \pi(\nu_{pump}) - (\tau_1 + \tau_2 - t') - \pi(\nu_{obs}) - \tau_2 - \text{echo}$$

A two-step phase cycling (+ $\langle x \rangle$, $-\langle x \rangle$) was performed on $\pi/2$ (ν_{obs}). Time t' is varied, whereas τ_1 and τ_2 are kept constant. The dipolar evolution time is given by $t = t' - \tau_1$. Data were analyzed only for $t > 0$. The resonator was overcoupled to $Q \approx 100$; the pump frequency ν_{pump} was set to the center of the resonator dip and coincided with the maximum of the nitroxide EPR spectrum, whereas the observer frequency ν_{obs} was ~65 MHz higher, coinciding with the low field local maximum of the spectrum. All measurements were performed at a temperature of 50 K with observer pulse lengths of 16 ns for $\pi/2$ and 32 ns for π pulses and a pump pulse length of 12 ns. Proton modulation was averaged by adding traces at eight different τ_1 values, starting at $\tau_{1,0}$ = 400 ns and increasing by increments of $\Delta\tau_1$ = 56 ns. Data points were collected in 8 ns time steps. The total measurement time for each sample was 8−24 h. Data analysis was performed with DeerAnalysis2011/2013.[42] For background correction in DeerAnalysis2011/2013, we considered distributions of the background spins with different dimensionalities, due to sample architecture. Considering the particles size (0.5−10 μm; see Figure 3), the surface topography may appear smooth to the protein molecule, which is approximately 10 nm in size. Thereby, for samples containing only protein in solution, a dimensional parameter D = 3 was used, while for solutions containing proteins attached on the BG substrates the dimensional parameter was D = 2.6. The last value was chosen considering that the protein is distributed in an approximately two dimensional layer on the BG surface after adsorption.

RESULTS AND DISCUSSION

Quantitative Adsorption Analysis Performed by cw-EPR Spectroscopy. The cw-EPR spectrum offers information about the spin concentration in the sample, which is directly proportional to the integrated EPR absorption signal. In this work, the absorption signal was used to calculate the amount of the protein attached on the BG. The data shown in Figure 4 reveals that after employing the ultrasonication procedure approximately 30% of the protein is removed from the pristine BG (red bars: from 508 to 353 μM), while only 16.9% is removed from the GA-functionalized BG (blue bars: from 491 to 408 μM). Although the MnmE concentrations on both BG substrates are nearly the same immediately after immersion, the ultrasonication process removes more protein from the pristine BG, indicating stronger protein attachment on the GA functionalized surface (Figure 4). A recent study performed on hemoglobin has also shown that the protein layer assembled on GA-functionalized BG does not cover the surface randomly but that the proteins bind only to specific sites on the surface,

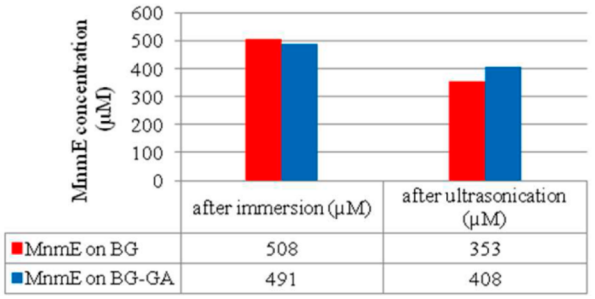

Figure 4. Concentration of MnmE adsorbed on pristine (BG) and GA-functionalized (BG-GA) bioactive glass, determined immediately after immersion and after ultrasonication. Errors are estimated to be ±10%, due to experimental settings and uncertainties in baseline subtraction.

resulting in stronger interactions between the protein molecule and the solid surface.[36]

Protein Immobilization on the BG Substrate. *(a). Nucleotide Free State (Apo-State).* The cw EPR spectra recorded for all MnmE single mutants in solution can be described by the coexistence of two spectral components, related to mobile (M) and immobile (I) fractions of the spin label side chain (Figure 5). The immobile component arises from the EPR signal of a fraction of spin labels engaged in secondary and tertiary interactions which restrict their reorientational freedom (e.g., having the N−O group hydrogen bonded to the protein). The mobile component corresponds to the signal provided by spin labels that have less constraints in their surroundings and that are exposed to an aqueous environment. The relative populations of these two states are in thermodynamic equilibrium, with all four positions exhibiting a more pronounced mobile component (M) in solution. In the case of E287R1, the relatively high mobility reflects the motional flexibility of the spin label side chain located at the G domain surface, while the high mobility observed for S278R1 can be explained by its location in the loop region of switch II,[26] that exhibits a very high structural flexibility. For positions K95R1 and I105R1, decreased flexibility is observed, in agreement with the location of these positions in the interface between the N-terminal domains of the dimer.

The two spectral components are visible in the EPR spectra of all mutants after adsorption on both BG substrates. However, the equilibrium between the two corresponding states appears to be significantly shifted towards the immobile component (I), suggesting that the environments of all residues are perturbed by the adsorption process. Consequently, all spectra recorded in the adsorbed state exhibit also an increase in the width of the central resonance line besides the increased amplitudes of the low field resonance line representing the immobile component (Figure 5). These changes correspond to a significant decrease of the spin label side chain mobility as a consequence of protein immobilization onto the BG surface. The extreme immobilization displayed by the spin labels attached at the two positions on the G domain (E287R1 and S278R1) is likely to appear due to direct interaction of this region with the BG surface, suggesting that these two positions may be located close to the contact points of the protein on the BG surface. This assumption is further supported by the spectra recorded on the GA functionalized substrate, revealing slightly stronger attachment of this region when the BG surface is covered with GA (Figure 5). Strikingly, the spin label attached

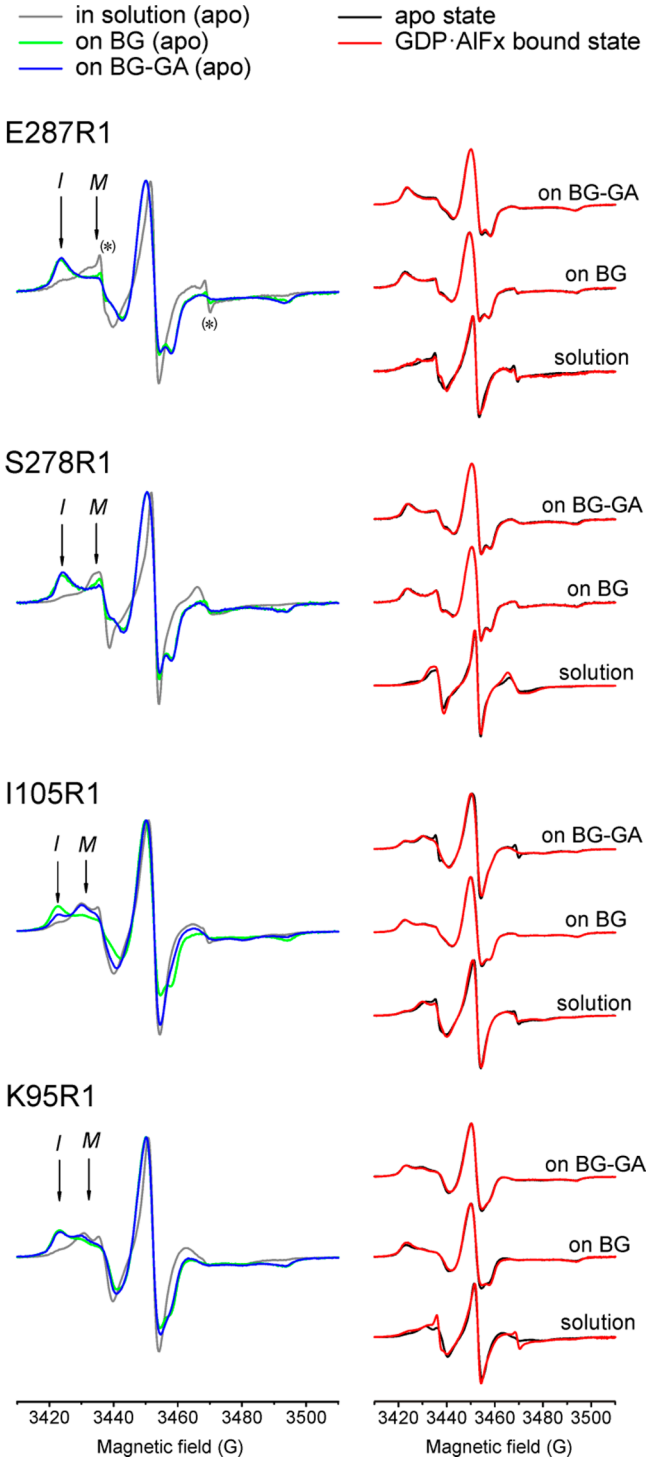

Figure 5. Left column: room temperature cw-EPR spectra of the spin labeled MnmE mutants E287, S278, I105, and K95 in solution (gray) and in adsorbed state (blue: on pristine BG; green: on GA functionalized BG). The mobile and immobile components are indicated by arrows and denoted with *M* and *I*, respectively. The peak in the spectrum of E287R1 marked by an asterisk (∗) corresponds to remaining unbound spin label in solution. Right column: superposition of the cw-EPR spectra recorded for the each MnmE mutant in the apo-state (black) and the GDP·AlF$_x$ bound state (red), in solution and after adsorption on the pristine (BG) and GA functionalized bioactive glass (BG-GA).

to position I105 exhibits higher mobility on the substrate functionalized with GA (Figure 5), pointing out that some local structural changes may occur upon adsorption on this substrate, e.g., a slight separation of this part of the N-terminal domains, allowing increased mobility of the I105R1 location. Accordingly, the other spin labeled position in the N-terminal domain (K95R1) should exhibit the same behavior. Indeed, an increased mobility is also observed for a spin label attached at position K95 after adsorption on GA functionalized BG, compared to the pristine substrate; nevertheless, the effect is smaller compared to the change of mobility exhibited by position I105 on the same substrates (Figure 5). The different response of position K95R compared to 105R1 upon adsorption on this substrate can be due to a local structural effect, as a consequence of the adsorption process. However, we do not exclude the possibility of a direct interaction of this site with the GA molecules from the bioactive glass surface, giving their high affinity towards lysine residues.[43] Since K95 is situated on an α-helix containing two lysine residues, both located in its close proximity (Figure 6), it appears to be likely that the interaction of GA molecules with the amino groups of these residues induces some restrictions in the helix mobility.

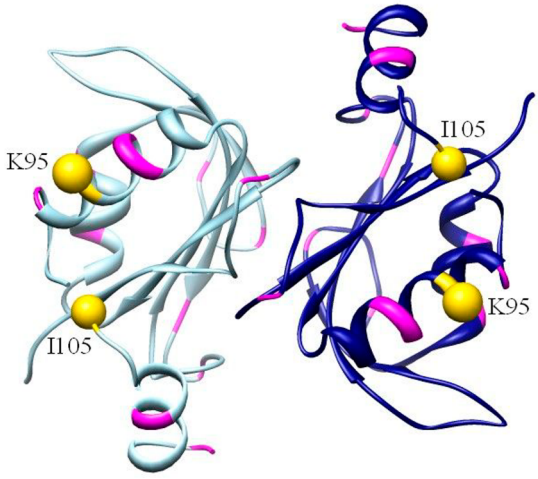

Figure 6. Location of positions K95 and I105 in the upper part of the N-terminal domains. The positions of the lysine residues mentioned in the text are marked in magenta.

(b). GDP·AlF$_x$ Bound State. Upon addition of GDP·AlF$_x$ in solution, the mobile component dominates the shape of the cw-EPR low-field spectral line for the S278R1 mutant, indicating certain flexibility of the R1 side chain. On the contrary, the intensity of the mobile component becomes less pronounced for the E287R1 variant, suggesting some restrictions for motion of the spin label side chain (see inset in Figure 5).

After adsorption on the BG, the striking similarity of the spectra recorded for the S278R1 and E287R1 mutants before and after GDP·AlF$_x$ addition (Figure 5) suggests that no significant conformational changes in the vicinity of the spin label side chains take place. This is in line with the G domain being strongly immobilized after adsorption and further supports our assumption that these two positions are close to contact points of the protein with the BG surface.

For positions K95 and I105, only small changes in their environment during the GTPase cycle are observed in solution, in line with their location in the N-terminal domains comprising a rigid dimerization domain. After attachment

dx.doi.org/10.1021/am500933e | ACS Appl. Mater. Interfaces 2014, 6, 7615−7625

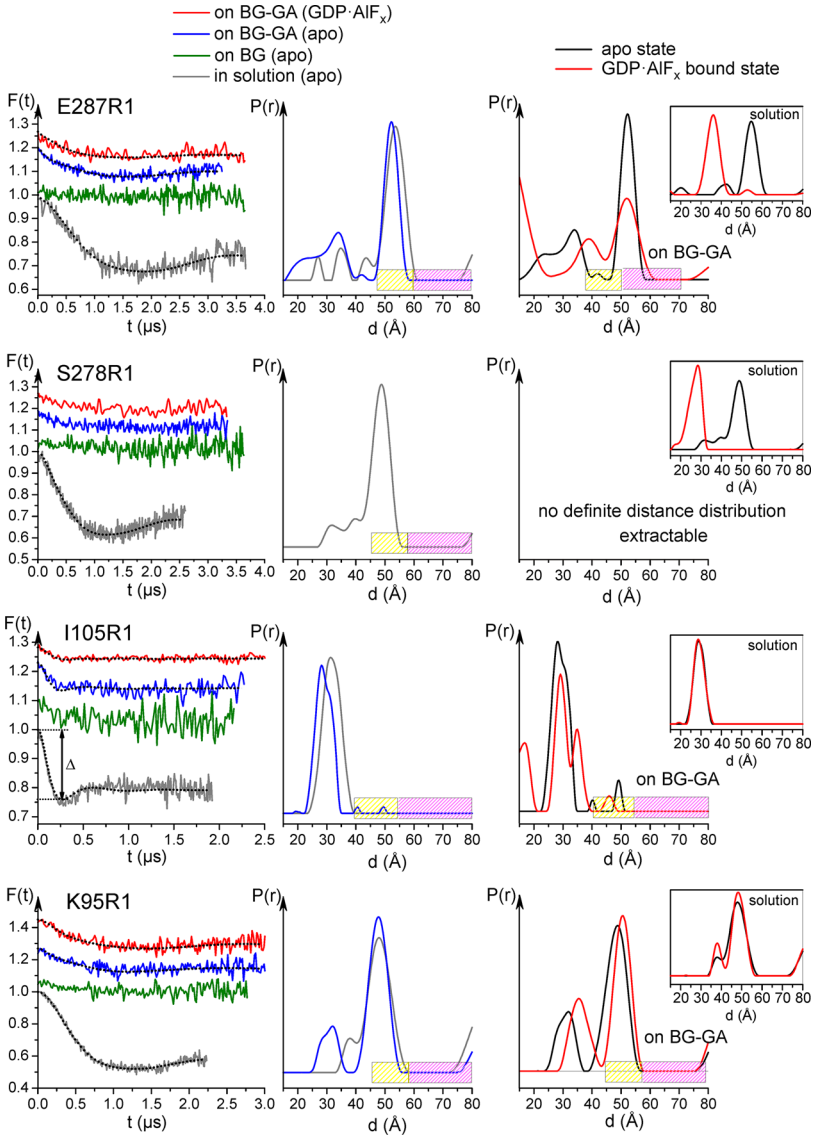

Figure 7. DEER characterization of MnmE single mutants in the apo-state: left panel, background corrected dipolar evolution data; middle panel, distance distributions obtained by Tikhonov regularization; right panel, comparison of distance distribution obtained for each MnmE single mutant in the apo-state (black) and the GDP·AlF$_x$ bound state (red) after adsorption on the GA functionalized BG (BG-GA). Inset: Same comparison in solution. Dotted lines in the left panels are fits to the data obtained by Tikhonov regularization. Colored boxes illustrate the reliability of the distance data: white = mean distance and shape of the distribution are reliable; light yellow = approximate distance but no information about the shape of the distribution; light magenta = no reliable predictions possible. The weak dipolar interaction displayed by the DEER traces recorded for the S278R1 mutant adsorbed on both substrates does not allow one to obtain a definite distance distribution (see text and the validation data shown in the Supporting Information).

onto the BG substrate, both positions also do not show significant changes upon addition of GDP·AlF$_x$ (Figure 5).

Conformational Changes Observed by DEER Spectroscopy. Pulse EPR experiments (DEER) were conducted to determine distance distributions between spin labels in native and adsorbed MnmE in order to compare protein dynamics by means of the observed distance distribution widths and to identify possible conformational changes induced in the protein structure upon attachment onto the BG substrate.

All DEER experiments were performed using deuterated buffer in order to improve the sensitivity and the maximum accessible distance range. Considering that the magnetic moment of deuterons is approximately 6.5 times smaller than the magnetic moment of protons, the fluctuations of the hyperfine field at the electron spin are significantly decreased in the case of deuterated solvents. This leads to a longer spin–spin relaxation time of nitroxide labels (the so called "phase memory time"), and accordingly, the maximum evolution time is prolonged.[41]

As previously shown,[26] the distance distributions obtained from DEER analyses of the MnmE-mutants E287R1 and S278R1, situated in the G domain, revealed that in solution the inter spin distances are significantly shorter in the presence of the GTP-hydrolysis transition state mimic[44] GDP·AlF$_x$ (36 Å for E287R1 and 28 Å for S278R1) compared with the apo-state (54 Å for E287R1 and 49 Å for S278R1) (Figure 7, Table 1). Consequently, the G domains in solution adopt an "open" conformation for the apo-state and a "closed" conformation for the GDP·AlF$_x$ bound state (see Figure 1), thereby assembling the catalytic machinery.[21] The nucleotide binding domains are

Table 1. Maxima in the Distance Distributions for the Pair of Spin Labels for Single MnmE Mutants in Solution and in the Adsorbed State, for Both G Domain Conformations[a]

label position	apo solution	apo BG-GA	GDP·AlF$_x$ solution	GDP·AlF$_x$ BG-GA
E287R1	**54**, 35	**52**, 34	**36**	**52**, 39
S278R1	**49**, 40, 32		**28**	
I105R1	**29**	**28**	**29**	**29**, 35
K95R1	**47**, 38	**48**	**48**, 38	**49**, 36

[a]The bold values correspond to the major maxima in the distance distributions.

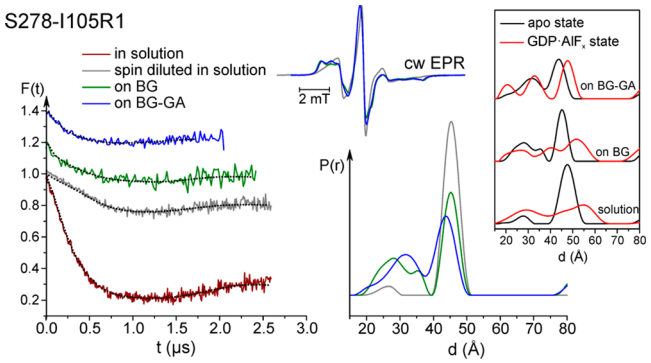

Figure 8. DEER data and cw-EPR spectra (top inset) recorded for the MnmE double mutant I105R1-S278R1 in the apo-state in solution (non-diluted and spin diluted sample) and after adsorption on both BG substrates. Left column: dipolar evolution time traces, showing comparable modulation depth for all three samples; right column: respective distance distributions of the doubly labeled MnmE mutant. All plots in the right column are normalized by amplitude.

thus highly mobile elements, capable of moving independently with regard to the other domains when the protein goes from the apo-state towards the GTP hydrolysis transition state. On the contrary, the other mutants investigated in this study, with R1 side chains located in the N-terminal domain, evidenced no (I105R1) or only minor (K95R1) changes in the distance distributions during the GTPase cycle. Position I105 exhibits a single population maximum at 29 Å for both states; the distance distributions of position K95 obtained for the apo-state (47 Å) and GDP·AlF$_x$ bound state (48 Å) reveals a slight shift of the major peak of about 1 Å, which is at the limit of the experimental accuracy (Figure 7, Table 1).

The DEER analyses of the samples containing MnmE adsorbed on BG reveal, at first glance, the extremely low modulation depth of the DEER traces recorded for singly labeled MnmE (~0 for all samples containing non-functionalized BG and <0.18 for samples containing GA functionalized BG), pointing out that only a very small number of spin label side chains exhibit dipolar interaction. Two hypotheses can be considered to explain this observation: (a) dissociation of most of the protein dimers involved in the adsorption process or (b) agglomeration of the protein layer on the BG surface. Accordingly, the low modulation depth is caused either by distances larger than ~6 nm between the two spin labels (according to the first assumption) or by a dense homogenous spatial distribution of the spin labels in the sample leading to intermolecular interactions (according to the second assumption).

In order to clarify this issue, further experiments were conducted with samples containing a MnmE double mutant (I105R1-S278R1) adsorbed on the BG. Spin dilution experiments were performed by mixing the MnmE double mutant with a 3-fold excess of non-labeled MnmE, and the DEER data obtained from these samples was compared to that obtained from the non-diluted sample. Since the distance between positions S278 and I105 within the MnmE monomer is in the DEER experimental range, a non-zero value of the modulation depth after adsorption would sustain the first assumption (dissociation of the MnmE dimer), while a value close to zero would confirm the second assumption (protein agglomeration).

The results shown in Figure 8 reveal that the modulation depths of the DEER traces recorded in the adsorbed state on both substrates are similar to the one recorded for the spin diluted sample in solution, sustaining the hypothesis of protein dissociation in two monomers as a consequence of interaction with the BG substrate. Proofing protein attachment, the cw-EPR spectrum recorded after adsorption showed that the equilibrium between the two spectral components mentioned before weighs in favor of the immobile component (Figure 8). The distance distributions obtained for the double mutant after interaction with the BG substrates exhibits two peaks, the major one at 45 Å being similar to the one observed also in solution (48 Å). As deduced from comparison with the distance distributions for the respective single mutants, this peak most likely arises from two different interactions: between the spin pair S278R1-S278R1′ within the protein dimer and between I105R1 and S278R1 within each monomer. After adsorption, assuming dimer dissociation, only the pair I105R1-S278R1 would contribute to this distance peak, justifying thus the observed small distance change. Remarkably, a second broad distance peak, ranging from 25 to 35 Å, appears after adsorption on the BG. Since the DEER experiments performed on the single mutant I105R1 adsorbed onto the pristine BG revealed a modulation depth of zero, implying dimer dissociation, it appears most likely that this broad peak solely represents the intramolecular distance between the I105R1-S278R1 pairs within the monomers. We conclude that adsorption onto the BG substrate induces not only dimer dissociation but also domain motions leading to a conformation where the G domain and the N-terminal domain of the monomers come into closer vicinity after adsorption. One possible explanation would be that the molecules contact the BG surface not only with their G domains but also with their N-terminal domains. Nevertheless, conformational changes within the G domains attached to the BG could also lead to changes in the domain arrangement of the protein. We favor the first assumption, as this would also directly explain the strong immobilization, being comparable to that seen for positions 278 and 287 in the G domains, observed for spin labels at positions I105 and K95 in the N-terminal domain on the pristine BG (see Figure 5).

Alternative control experiments were performed with the single mutant S278R1: the protein was brought to its closed conformation (by the addition of GDP·AlF$_x$ in solution) and subsequently subjected to the adsorption process on the pristine BG (Figure 9). The dominant immobile component observed in the cw EPR spectrum again indicates an extreme immobilization of spin labels at this position on the BG substrate. In addition, the modulation depth of almost zero in the DEER trace recorded after adsorption suggests a largely increased gap between the two switch II regions after adsorption, further sustaining the hypothesis of MnmE

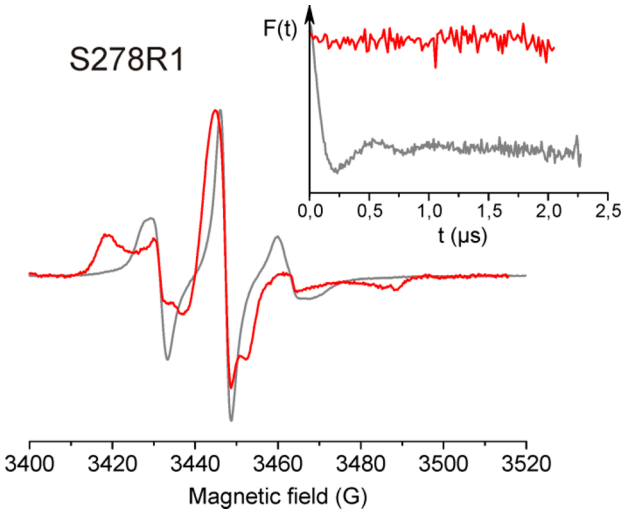

Figure 9. cw-EPR spectra and DEER dipolar evolution time traces (inset) recorded for the spin labeled mutant S278, in GDP·AlF$_x$ bound state, in solution (gray lines) and after adsorption (red lines) on the pristine bioactive glass.

dissociation as result of the adsorption process, even if an additional dimerization interface is composed by the G domains in the transition state. Thus, it can be concluded that the interaction between the protein and the BG substrate is significantly stronger compared to the protein−protein interaction in the MnmE dimer. Finally, additional DEER experiments conducted on spin diluted MnmE-E287R1 and S278R1 (data not shown) revealed zero modulation depth for spectra recorded on samples in the BG-adsorbed state, thus also excluding the hypothesis of protein agglomeration as a cause for the observed low modulation depths.

Effects of GA Functionalization. Notably, for the single mutants, DEER traces being analyzable in terms of inter spin distances could be obtained for the samples containing GA-functionalized BG (but not for those with non-functionalized BG), suggesting that a small fraction of the protein still keeps its dimeric state after adsorption onto this substrate. In fact, previous studies have shown that protein coupling agents can help in maintaining the native protein structure upon adsorption.[28,45,46]

Information about the fraction of interacting spins after adsorption (i.e., the fraction of proteins that do not dissociate as a consequence of the adsorption process) can be inferred from the modulation depth values of the DEER time traces.[40,41,47] The fraction of remaining interacting spins on the GA functionalized substrate, relative to the proteins in solution, was determined for the single mutants E287R1, I105R1, and K95R1. The number of interacting spins per protein molecule can be determined from the relation:

$$N = \frac{\ln(1 - \Delta)}{1 - \lambda} + 1 \quad (1)$$

where Δ is the modulation depth of the background corrected DEER time trace (see Figures 7 and 8) and λ is a spectrometer-dependent parameter. In the present study, the purpose of our experiments was to determine the number of the remaining interacting spins after adsorption on the BG substrate with respect to the number of interacting spins in solution. In a particularly simple approach that does not require exact knowledge of spin labeling efficiencies or dissociation constants, this can be calculated by the following equation:

$$N_{\text{BG-relative}} = \frac{\ln(1 - \Delta_{\text{BG-GA}})}{\ln(1 - \Delta_{\text{sol}})} + 1 \quad (2)$$

where Δ_{sol} and $\Delta_{\text{BG−GA}}$ are the modulation depths of the background corrected DEER traces recorded before and after adsorption of the protein on the BG substrate.

The modulation depth values Δ determined from the background corrected DEER time traces of MnmE-E287R1, -I105R1, and -K95R1 and the corresponding relative numbers of interacting spin pairs after adsorption on the GA functionalized BG are given in Table 2.

Table 2. Modulation Depth Values Δ, Determined from the Background Corrected DEER Time Traces of the E287R1, I105R1, and K95R1 Mutants, the Relative Number of Interacting Spin Pairs (N), and the Percentage of Intact MnmE Dimers after Adsorption on the GA Functionalized Substrate

label position	state	Δ	N	% dimers
E287R1	in solution	0.32	1.33	66
	adsorbed	0.12		
I105R1	in solution	0.25	1.34	67
	adsorbed	0.095		
K95R1	in solution	0.47	1.25	63
	adsorbed	0.145		

The relative numbers of interacting spins correspond to ∼65% of the number of interacting spins observed in solution. This result indicates that on the GA functionalized substrate about 2/3 of the MnmE molecules are still dimers. For this fraction, in case of the mutants E287R1, I105R1, and K95R1, distance distributions have been obtained after adsorption onto the GA functionalized BG. For the apo-state, these distance distributions obtained after adsorption of the protein on the substrate are approximately the same compared to the corresponding ones obtained in solution (Figure 7, Table 1), suggesting that the two G domains adopt the open conformation after adsorption.

Upon addition of GDP·AlF$_x$, the distance distribution obtained in the adsorbed state for MnmE-E287R1 was the same as that obtained in the apo-state (major peak at 52 Å), suggesting that the G domains of MnmE even in the presence of the transition state mimic GDP·AlF$_x$ remain in the open conformation. It seems that after adsorption the protein is "locked" in the open state and consequently will not be able to accomplish its biological function anymore. The immobilization of MnmE in the open state confirms also the hypothesis brought up on the basis of the cw experiments, namely, that the top of the G domains comprise the contact region of the protein with the BG substrate.

Positions K95R1 and I105R1 in the N-terminal domain of MnmE are also affected by GTP hydrolysis, since both positions display major distance maxima that are shifted towards higher values compared to the apo-state (Figure 7, Table 1). In addition, a new maximum at larger distances (35 Å) appears in the distance distribution of I105R1 in the GDP·AlF$_x$ bound state, which might be associated with separation of the two N-terminal domains as a consequence of interaction between the protein molecules and the GA functionalized BG.

This separation would also explain the increase in spin label mobility revealed from the cw-EPR spectrum of I105R1 when the protein is adsorbed on the GA functionalized BG (Figure 5).

The MnmE-mutant S278R1 appears as a special case: even on the GA functionalized BG, the spin labels attached at this position seem to be too far apart from each other to be detectable by the DEER experiment (Figure 7). Keeping the location of position 278 in the switch II region of the G domain, an extended loop structure (see Figure 1), in mind, it can easily be envisioned that interaction with the BG substrate could induce large-scale conformational changes of such flexible regions. Obviously, adsorbed onto the BG substrate, the protein adopts a conformation in which the two positions 278 are situated at a significantly larger distance (>70−80 Å) compared to the structure in solution. We speculate that this loop region represents an anchoring point of the protein on the BG surface, the two 278 positions being pulled to opposite directions as a consequence of the protein spreading onto the surface.

Consequently, despite the fact that in contrast to pristine BG about 2/3 of the MnmE molecules do not dissociate after adsorption on the GA-functionalized BG substrate, the functionality of the protein appears to be severely impaired. We assume that GA decreases the surface hydrophobicity and acts as buffer between the protein molecules and the bioactive glass surface, making the adsorption process less aggressive on this substrate than on the pristine BG, but it still might severely affect functionality of the adsorbed biomolecule as the protein−substrate interaction appears to be stronger than the protein−protein interactions.

Figure 10 schematically depicts the results presented above. We assume that upon adsorption of MnmE onto the pristine BG (panel B) the dimers dissociate and the resulting monomers rearrange so that the G and N-terminal domains come in contact with the BG surface. These two regions display enhanced interaction with the substrate, since the hydrophobic domains of MnmE are mostly located in the inner parts of its three dimensional structure, which are mainly situated in the G domain and the N-terminal domain of the protein (Figure 11). It remains questionable if the helical domain spreads onto the surface or if it dangles in solution. On the basis of the fact that this region displays a mainly hydrophilic surface (see Figure 11), one plausible hypothesis would be that it does not interact strongly with the BG. However, in a previous study, we have shown that MnmE loses approximately half of its α-helical structure upon adsorption on this type of substrate.[28] Further EPR investigations on MnmE spin labeled at positions in the helical domain are needed to clarify this issue. On the GA-functionalized surface (Figure 10C), about 2/3 of the MnmE molecules are still dimeric, but interaction of the G domains with the substrate hampers G domain dimerization in the GTP hydrolysis transition state as described in the previous sections.

CONCLUSIONS

Surface bioactivity of implants, BG is commonly used as a biomaterial for bone defects repair, is provided by the adsorbed protein layer. The types and the amount of proteins adsorbed, as well as their orientation, conformation, and packing density, are determinants for cell attachment and consequently for biocompatibility of the material. Accordingly, to control cellular response, it is important to first understand how surface chemistry and surface topology influence the formation of the

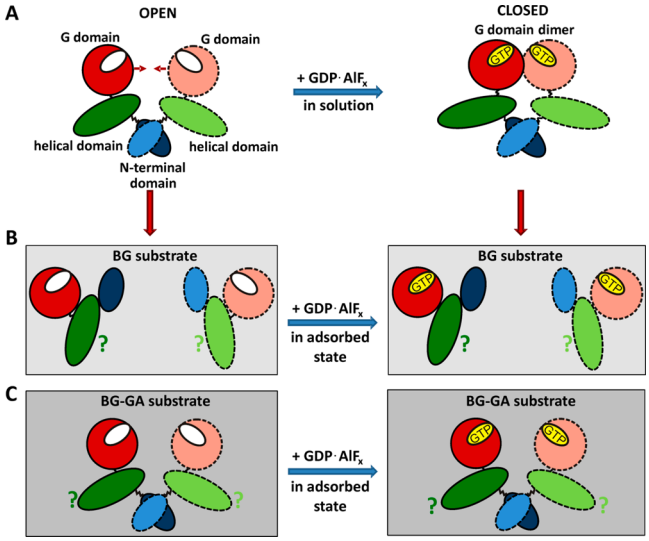

Figure 10. Schematic illustration of activation of MnmE during GTP hydrolysis in solution and after adsorption on the bioactive glass (top view). (A) In solution, the G domains adopt an open conformation in the apo-state and a closed conformation in the GDP·AlF$_x$ bound state. (B) Upon adsorption on the pristine BG, the strong interaction between the protein molecule and the BG substrate leads to dimer dissociation; the question marks emphasize that no information is available regarding the helical domain behavior, since no data were recorded for this region of the protein. (C) The protein coupling agent GA mediates the interaction between the protein molecules and the hydrophobic surface of the bioactive glass, so that a fraction of 65% protein molecules keeps its dimeric form on the GA functionalized substrate. On both substrates, the G domains are in contact with the BG substrate and, consequently, remain open after addition of GDP·AlF$_x$.

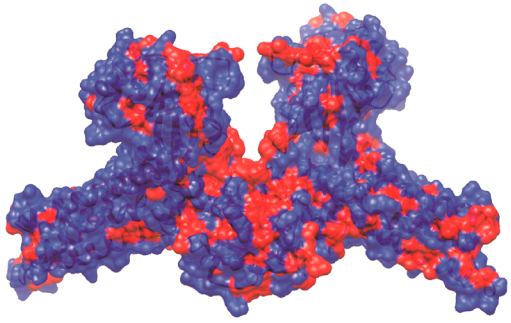

Figure 11. Structure of MnmE (pdb code 1XZP). The hydrophobic and hydrophilic domains are depicted in red and blue, respectively.

adsorbed protein layer and the bioactive sites presented by this layer.[14]

EPR spectroscopy and site-directed spin labeling were employed in this work to explore the interaction of the tRNA-modifying enzyme MnmE from *E. coli*, an ortholog of the human enzyme hGTPBP3, with the BG surface in terms of quantitative analysis, protein immobilization, and conformational changes. Our results reveal that adsorption onto the pristine bioactive glass surface causes full dissociation of the functional GTPase dimers, resulting in complete functional impairment (full functionality of the enzyme requires binding of another dimeric protein, GidA, in the vicinity of the N-terminal domains in order to promote GTPase activity and tRNA modification[48]), as the contact regions to the BG are the G domain and the N-terminal domain.

Contrarily, a fraction of ∼65% of the protein keeps its dimeric form if the BG surface is functionalized with GA. This protein coupling agent seems to mediate the interaction between the protein molecules and the hydrophobic surface of the bioactive glass, leading to a less aggressive interaction between the protein domains and the BG substrates. Nevertheless, the large conformational change observed for MnmE in solution upon GTP hydrolysis does not occur when the protein is attached to the functionalized BG substrate, suggesting that the protein is "locked" in the open state as a consequence of strong immobilization of both G domains onto the BG-GA surface. Our analyses of the conformational changes taking place upon adsorption of MnmE on the GA-functionalized BG reveal characteristics of the interactions taking place that are easily transferable to other protein structures, especially to multi-domain enzymes where large-scale conformational changes take place in the course of the catalytic cycle, thus providing further insights into protein adsorption onto pristine and functionalized bioactive glasses in general.

■ ASSOCIATED CONTENT

Ⓢ Supporting Information

X-ray diffraction (XRD) and Fourier-transform IR (FTIR) spectroscopy; DEER data validations. This material is available free of charge via the Internet at http://pubs.acs.org.

■ AUTHOR INFORMATION

Corresponding Author

*E-mail: johann.klare@uos.de. Tel.: +49 541 969 2664. Fax: +49 541 969 2656.

Author Contributions

The manuscript was written through contributions of all authors. All authors have given approval to the final version of the manuscript.

Funding

This work was supported by the Deutsche Forschungsgemeinschaft, Grant KL2077/1-1. Support by the DAAD programme "Ostpartnerschaften" is gratefully acknowledged.

Notes

The authors declare no competing financial interest.

■ ACKNOWLEDGMENTS

We acknowledge A. Wittinghofer, S. Meyer, and A. Krueger from the Max Planck-Institute for molecular physiology (Dortmund, Germany) for providing some of the MnmE preparations.

■ ABBREVIATIONS

APTS, 3-aminopropyl-triethoxysilane
BG, bioglass
cw, continuous wave
DEER, double electron-electron resonance
EPR, electron paramagnetic resonance
GA, glutaraldehyde
GDP, guanosine diphosphate
GTP, guanosine triphosphate
MTSSL, methanethiosulfonate spin label
SDSL, site-directed spin labeling

■ REFERENCES

(1) Servagent-Noinville, S.; Revault, M.; Quiquampoix, H.; Baron, M.-H. Conformational Changes of Bovine Serum Albumin Induced by Adsorption on Different Clay Surfaces: FTIR Analysis. *J. Colloid Interface Sci.* **2000**, *221*, 273−283.

(2) Dousseau, F.; Pezolet, M. Determination of the Secondary Structure Content of Proteins in Aqueous Solutions from Their Amide I and Amide II Infrared Bands. Comparison between Classical and Partial Least-Squares Methods. *Biochemistry* **1990**, *29*, 8771−8779.

(3) Wang, K.; Zhou, C.; Hong, Y.; Zhang, X. A Review of Protein Adsorption on Bioceramics. *Interface Focus* **2012**, *2*, 259−277.

(4) Sawyer, A.; Hennessy, K.; Bellis, S. Regulation of Mesenchymal Stem Cell Attachment and Spreading on Hydroxyapatite by RGD Peptides and Adsorbed Serum Proteins. *Biomaterials* **2005**, *26*, 1467−1475.

(5) Radin, S.; Ducheyne, P. Effect of Serum Proteins on Solution-Induced Surface Transformations of Bioactive Ceramics. *J. Biomed. Mater. Res.* **1996**, *30*, 273−279.

(6) Langstaff, S.; Sayer, M.; Smith, T. J.; Pugh, S. M. Resorbable Bioceramics Based on Stabilized Calcium Phosphates. Part II: Evaluation of Biological Response. *Biomaterials* **2001**, *22*, 135−150.

(7) Kotani, S.; Yamamuro, T.; Nakamura, T.; Kitsugi, T.; Fujita, Y.; Kawanabe, K.; Kokubo, T. Enhancement of Bone Bonding to Bioactive Ceramics by Demineralized Bone Powder. *Clin. Orthop. Relat. Res.* **1992**, *278*, 226−234.

(8) Fujita, Y.; Yamamuro, T.; Nakamura, T.; Kitsugi, T.; Kotani, S.; Ohtsuki, C.; Kokubo, T. Mechanism and Strength of Bonding Between Two Bioactive Ceramics in Vivo. *J. Biomed. Mater. Res.* **1992**, *26*, 1311−1324.

(9) Mavropoulos, E.; Costa, A. M.; Costa, L. T.; Achete, C. A.; Mello, A.; Granjeiro, J. M.; Rossi, A. M. Adsorption and Bioactivity Studies of Albumin onto Hydroxyapatite Surface. *Colloids Surf., B: Biointerfaces* **2011**, *83*, 1−9.

(10) Bender, S. A.; Bumgardner, J. D.; Roach, M. D.; Bessho, K.; Ong, J. L. Effect of Protein on the Dissolution of HA Coatings. *Biomaterials* **2000**, *21*, 299−305.

(11) Wang, K.; Leng, Y.; Lu, X.; Ren, F.; Ge, X.; Ding, Y. Theoretical Analysis of Protein Effects on Calcium Phosphate Precipitation in Simulated Body Fluid. *CrystEngComm* **2012**, *14*, 5870−5878.

(12) Wang, K.; Zhou, C.; Hong, Y.; Zhang, X. A Review of Protein Adsorption on Bioceramics. *Interface Focus* **2012**, *2*, 259−277.

(13) Sanz-Herrera, J. A.; Boccaccini, A. R. Modelling Bioactivity and Degradation of Bioactive Glass Based Tissue Engineering Scaffolds. *Int. J. Solids Struct.* **2011**, *48*, 257−268.

(14) Latour, R. A., Jr. Biomaterials: Protein-Surface Interactions. In *Encyclopedia of Biomaterials and Biomedical Engineering*; Informa Healthcare: New York, 2005; pp 1−15.

(15) Altenbach, C.; Marti, T.; Khorana, H. G.; Hubbell, W. L. Transmembrane Protein Structure: Spin Labeling of Bacteriorhodopsin Mutants. *Science* **1990**, *248*, 1088−1092.

(16) Bordignon, E.; Steinhoff, H.-J. Membrane Protein Structure and Dynamics Studied by Site-Directed Spin Labeling ESR. In *ESR Spectroscopy in Membrane Biophysics*; Hemminga, M. A.; Berliner, L. J., Eds.; Springer Science and Business Media: New York, 2007; pp 129−164.

(17) Klare, J. P.; Steinhoff, H.-J. Spin Labeling EPR. *Photosynth. Res.* **2009**, *102*, 377−390.

(18) Klare, J. P. Site-Directed Spin Labeling EPR Spectroscopy in Protein Research. *Biol. Chem.* **2013**, *394*, 1281−1300.

(19) Gasper, R.; Meyer, S.; Gotthardt, K.; Sirajuddin, M.; Wittinghofer, A. It Takes Two to Tango: Regulation of G Proteins by Dimerization. *Nat. Rev. Mol. Cell Biol.* **2009**, *10*, 423−429.

(20) Agris, P. F.; Vebdeix, F. A.; Graham, W. D. tRNA's Wobble Decoding of the Genome: 40 Years of Modification. *J. Mol. Biol.* **2007**, *366*, 1−13.

(21) Li, X.; Guan, M. X. A Human Mitochondrial GTP Binding Protein Related to tRNA Modification May Modulate Phenotypic Expression of the Deafness-Associated Mitochondrial 12S rRNA Mutation. *Mol. Cell. Biol.* **2002**, *22*, 7701−7711.

(22) Suzuki, T.; Suzuki, T.; Wada, T.; Saigo, K.; Watanabe, K. Taurine as a Constituent of Mitochondrial tRNAs: New Insights into

the Functions of Taurine and Human Mitochondrial Diseases. *EMBO J.* **2002**, *21*, 6581−6589.
(23) Villarroya, M.; Prado, S.; Esteve, J. M.; Soriano, M. A.; Aguado, C.; Perez-Martínez, D.; Martínez-Ferrandis, J. I.; Yim, L.; Victor, V. M.; Cebolla, E.; Montaner, A.; Knecht, E.; Armengod, M. E. Characterization of Human GTPBP3, a GTP-Binding Protein Involved in Mitochondrial tRNA Modification. *Mol. Cell. Biol.* **2008**, *28*, 7514−7531.
(24) Bykhoskaya, Y.; Mengseha, E.; Wang, D.; Yang, H.; Estivill, X.; Shohat, M.; Fischel-Godsian, N. Phenotype of Non-Syndromic Deafness Associated with the Mitochondrial A1555G Mutation is Modulated by Mitochondrial RNA Modifying Enzymes MTO1 and GTPBP3. *Mol. Genet. Metab.* **2004**, *83*, 199−206.
(25) Scrima, A.; Vetter, I. R.; Armengod, M. E.; Wittinghofer, A. The Structure of the TrmE GTP-Binding Protein and its Implications for tRNA Modification. *EMBO J.* **2005**, *24*, 23−33.
(26) Meyer, S.; Böhme, S.; Krüger, A.; Steinhoff, H.-J.; Klare, J. P.; Wittinghofer, A. Kissing G Domains of MnmE Monitored by X-ray Crystallography and Pulse EPR Spectroscopy. *PLoS Biol.* **2009**, *7*, No. e1000212.
(27) Scrima, A.; Wittinghofer, A. Dimerisation-Dependent GTPase Reaction of MnmE: How Potassium Acts as GTPase-Activating Element. *EMBO J.* **2006**, *25*, 2940−2951.
(28) Gruian, C.; Vanea, E.; Simon, S.; Simon, V. FTIR and XPS Studies of Protein Adsorption onto Functionalized Bioactive Glass. *Biochim. Biophys. Acta* **2012**, *1824*, 873−881.
(29) El-Ghannam, A.; Ducheyne, P.; Shapiro, I. M. Effect of Serum Proteins on Osteoblast Adhesion to Surface-Modified Bioactive Glass and Hydroxyapatite. *J. Orthop. Res.* **1999**, *17*, 340−345.
(30) Chen, Q. Z.; Rezwan, K.; Armitage, D.; Nazhat, S. N.; Boccaccini, A. R. The Surface Functionalization of 45S5 Bioglass-Based Glass-Ceramic Scaffolds and Its Impact on Bioactivity. *J. Mater. Sci. Mater. Med.* **2006**, *17*, 979−987.
(31) Chen, Q. Z.; Rezwan, K.; Françon, V.; Armitage, D.; Nazhat, S. N.; Jones, F. H.; Boccaccini, A. R. Surface Functionalization of Bioglass-Derived Porous Scaffolds. *Acta Biomater.* **2007**, *3*, 551−562.
(32) Hubbell, W. L.; Altenbach, C. Investigation of Structure and Dynamics in Membrane Proteins Using Site-Directed Spin Labelling. *Curr. Opin. Struct. Biol.* **1994**, *4*, 566−573.
(33) Jacobsen, K.; Oga, S.; Hubbell, W. L.; Risse, T. Determination of the Orientation of T4 Lysozyme Vectorially Bound to a Planar-Supported Lipid Bilayer Using Site-Directed Spin Labeling. *Biophys. J.* **2005**, *88*, 4351−4365.
(34) Risse, T.; Hubbell, W. L.; Isas, J. M.; Haigler, H. T. Structure and Dynamics of Annexin 12 Bound to a Planar Lipid Bilayer. *Phys. Rev. Lett.* **2003**, *91*, 188101.
(35) Vanea, E.; Gruian, C.; Rickert, C.; Steinhoff, H.-J.; Simon, V. Structure and Dynamics of Spin-Labeled Insulin Entrapped into Silica Matrix by Sol-Gel Method. *Biomacromolecules* **2013**, *14*, 2582−2592.
(36) Gruian, C.; Vulpoi, A.; Steinhoff, H.-J.; Simon, S. Structural Changes of Methemoglobin after Adsorption on Bioactive Glass, as a Function of Surface Functionalization and Salt Concentration. *J. Mol. Struct.* **2012**, *1015*, 20−26.
(37) Vulpoi, A.; Gruian, C.; Vanea, E.; Baia, L.; Simon, S.; Steinhoff, H.-J.; Göller, G.; Simon, V. Bioactivity and Protein Attachment onto Bioactive Glasses Containing Silver Nanoparticles. *J. Biomed. Mater. Res., Part A* **2012**, *100*, 1179−1186.
(38) Verne, E.; Vitale-Brovarone, C.; Bui, E.; Bianchi, C. L.; Boccaccini, A. R. Surface Functionalization of Bioactive Glasses. *J. Biomed. Mater. Res., Part A* **2009**, *90*, 981−992.
(39) Tunc, S.; Maitz, M. F.; Steiner, G.; Vazquez, L.; Pham, M. T.; Salzer, R. In Situ Conformational Analysis of Fibrinogen Adsorbed on Si Surfaces. *Colloids Surf., B* **2005**, *42*, 219−225.
(40) Pannier, M.; Veit, S.; Godt, A.; Jeschke, G.; Spiess, H. W. Dead-Time Free Measurement of Dipole-Dipole Interactions between Electron Spins. *J. Magn. Reson.* **2000**, *142*, 331−340.
(41) Jeschke, G.; Polyhach, Y. Distance Measurements on Spin-Labelled Biomacromolecules by Pulsed Electron Paramagnetic Resonance. *Phys. Chem. Chem. Phys.* **2007**, *9*, 1895−1910.
(42) Jeschke, G.; Chechik, V.; Ionita, V.; Godt, A.; Zimmermann, H.; Banham, J.; Timmel, C. R.; Hilger, D.; Jung, H. DeerAnalysis2006 - A Comprehensive Software Package for Analyzing Pulsed ELDOR Data. *Appl. Magn. Reson.* **2006**, *30*, 473−498.
(43) Migneault, I.; Dartiguenave, C.; Bertrand, M. J.; Waldron, K. C. Glutaraldehyde: Behavior in Aqueous Solution, Reaction with Proteins, and Application to Enzyme Crosslinking. *Biotechniques* **2004**, *37*, 790−806.
(44) Wittinghofer, A. Signaling Mechanistics: Aluminum Fluoride for Molecule of the Year. *Curr. Biol.* **1997**, *7*, R682−R685.
(45) Heule, M.; Rezwan, K.; Cavalli, L.; Gauckler, L. J. A Miniaturized Enzyme Reactor Based on Hierarchically Shaped Porous Ceramic Microstruts. *Adv. Mater.* **2003**, *15*, 1191−1194.
(46) Weetall, H. H. Enzymes Immobilized on Inorganic Supports. *Trends Biotechnol.* **1985**, *3*, 276−280.
(47) Bode, B. E.; Margraf, D.; Plackmeyer, J.; Dürner, G.; Prisner, T. F.; Schiemann, O. Counting the Monomers in Nanometer-Sized Oligomers by Pulsed Electron-Electron Double Resonance. *J. Am. Chem. Soc.* **2007**, *129*, 6736−6745.
(48) Boehme, S.; Meyer, S.; Krueger, A.; Steinhoff, H.-J.; Wittinghofer, A.; Klare, J. P. Stabilization of G Domain Conformations in the tRNA Modifying MnmE/GidA Complex Observed with DEER Spectroscopy. *J. Biol. Chem.* **2010**, *285*, 16991−17000.